Colloid Polym Sci (2008) 286:1307–1315
DOI 10.1007/s00396-008-1898-7

ORIGINAL CONTRIBUTION

Convectional, sedimentation and drying dissipative patterns of colloidal crystals of poly(methyl methacrylate) spheres on a watch glass

Tsuneo Okubo

Received: 15 April 2008 / Accepted: 31 May 2008 / Published online: 12 July 2008

Abstract Direct observation of the convectional dissipative patterns at room temperature was successful on a cover glass during the course of dryness of colloidal crystals of poly(methyl methacrylate) colloidal spheres. Formation processes of the convectional patterns of spoke-like lines were observed as a function of sphere size and also sphere concentration. During dryness of the suspensions, the brilliant iridescent colors changed beautifully. Macroscopic and microscopic drying patterns of the dried film were observed. Multiple broad ring-like patterns were observed especially at low sphere concentrations. The water evaporation accompanied with the convectional flow of water and the colloidal spheres played an important role for the dissipative structure formation.

Keywords Poly(methyl methacrylate) colloids · Convectional pattern · Drying pattern · Dissipative structure · Spoke line · Broad ring · Watch glass

Introduction

Most structural patterns in nature are formed via self-organization accompanied with the dissipation of free energy and in the non-equilibrium state. Among several factors in the free energy dissipation of aqueous colloidal suspensions, evaporation of water molecules at the air–water interface and gravitational convection are very important. In order to understand the mechanisms of the dissipative self-organization of the simple model systems, instead of much complex nature itself, several research groups including us have studied the *convectional* [1–7], *sedimentation* [8–12], and *drying* dissipative patterns [13–51] during the course of drying suspensions and also solutions.

Interestingly, macroscopic *broad ring* drying patterns of the hills accumulated with solutes at the outside edge were formed for almost all solutes. For the nonspherical-shaped solutes, however, a central round hill was formed in the central area in addition to the broad rings. Macroscopic spoke lines, cracks, or fine hills including flickering spoke lines were also observed in the dried film for many solutes. Furthermore, so many types of microscopic drying patterns such as branch-like, arc-like, block-like, star-like, cross-like, string-like, and others were observed. It should be noted here that the macroscopic broad rings and spoke lines were observed already in the convectional and/or sedimentation patterns. The broad ring sedimentation patterns in the liquid phase were observed first in a previous paper from the author's laboratory [9], though the broad ring formation in the dried films has been reported so often. A main cause for the broad ring and spoke lines is due to the convectional flow of water and solutes mainly from the central area toward the outside edge in the lower layers of the liquid, which was observed directly from the movement of the reversibly occurred aggregates of the colloidal particles of Chinese black ink [1–3, 6]. Clearly, the convectional flow is enhanced by the evaporation of water at the liquid surface, resulting in lowering of the suspension and/or solution temperature in the upper region of the liquid. Magnitudes of

T. Okubo (✉)
Institute for Colloidal Organization,
Hatoyama 3-1-112,
Uji, Kyoto 611-0012, Japan
e-mail: okubotsu@ybb.ne.jp

T. Okubo
Cooperative Research Center, Yamagata University,
Johnan 4-3-16,
Yonezawa 992-8510, Japan

the temperature lowering at the liquid surface at 25°C compared with the bulk temperature were estimated to be 2°C with the humidity of air at 40% [5]. It should be mentioned further that the vague primitive patterns formed already in the liquid state before dryness, and they grew toward the fine structures during the course of solidification [38]. It should be further mentioned here that the theoretical studies for these convectional patterns using Navier–Stokes equations are not always successful yet [5, 52–56]. In most cases, the broad ring-like sedimentation structures form in between the convectional and drying patterns [7–12, 48, 50, 51]. It was clarified that the sedimentary spheres float from the substrates by the repulsions between the electrical double layers surrounding the colloidal spheres and the substrates. Furthermore, the sedimentary patterns were formed by the balancing between the upward movement of spheres by the convection flow and the downward sedimentation and quite sensitive to the surrounding temperature and humidity. The drying pattern method was clarified to be one of the new characterization techniques of colloidal mixtures [48, 50].

In a previous paper [51], the convectional spoke-line patterns were observed on a cover glass at room temperature successfully for colloidal crystal suspensions of poly (methyl methacrylate) (PMMA) spheres (100, 200, and 300 nm in diameter). The reason why the convectional patterns are visualized for PMMA system is due to the fact that the colloidal surfaces of PMMA spheres are weakly hydrophobic in aqueous suspension. It is highly plausible that the reversible and temporal aggregates of PMMA spheres are formed, and their convectional flows are visualized like Chinese black ink [6]. The other reason will be the partial and local melting of the colloidal crystals of PMMA by the convectional flow of water and solutes. In this work, the author studied the convectional patterns further on a watch glass. On the substrate, the clear convectional spoke-like lines were observed successfully at room temperature. Sedimentation patterns and also macroscopic and microscopic drying patterns of suspensions of PMMA spheres and their size, ranging from 100 nm to 1.0 μm, are studied in this paper.

Experimental

Materials

Poly(methyl methacrylate) (PMMA) spheres, GW1 (100± 7 nm in diameter and polydispersity index), GW6 (200± 10 nm), GW8 (300±12 nm), and PM1000 (1.0 μm±20 nm), were kindly donated from Soken Chemicals (Tokyo). These size parameters were determined on an electron microscope by the manufacturer. PM1000 spheres were carefully purified more than 30 times by decantation with pure water, since a large amount of the detergents used for sphere synthesis must be deleted from the stock suspension. Then, all the stock sample suspensions were treated on a mixed bed of cation- and anion-exchange resins [Bio-Rad, AG501-X8(D), 20–50 mesh] for more than 4 years before use. The stock suspensions from GW1 to PM1000 spheres thus obtained crystallized and emitted strong iridescent bluish to whitish colors, respectively. Water used for the sample preparation was purified by a Milli-Q reagent-grade system (Milli-RO5 plus and Milli-Q plus, Millipore, Bedford, MA, USA).

Observation of the dissipative structures

Four milliliters of the suspensions were put carefully and gently into a medium-size watch glass (70 mm in diameter, TOP, Tokyo). A disposable serological pipet (10 ml, Corning Lab Sci) was used for putting the suspension on a watch glass. The convectional, sedimentation, and drying patterns were observed for the suspensions on a desk covered with a black plastic sheet. The room temperature was regulated rat 24°C, 25°C, or 26°C. Humidity of the room was not regulated and between 45% and 60%. Sphere concentrations were between 0.0002 and 0.1 in volume fraction.

Macroscopic patterns were observed on a Canon EOS 10 D digital camera with a macro-lens (EF 50 mm, f=2.5) and a life-size converter EF. Microscopic drying patterns were observed with a metallurgical microscope (PME-3, Olympus, Tokyo). Thickness profiles of the dried films were measured on a laser 3D profile microscope (type VK-8500, Keyence, Osaka).

Results and discussion

Convectional patterns on a watch glass

Figure 1 shows the typical examples of the convectional patterns of GW1 (Fig. 1a,b), GW6 (Fig. 1c,d), and GW8 (Fig. 1e,f) spheres, respectively. The convectional patterns were not observed for PA1000 spheres, which will be due to the strong multi-scattering of light. At a first glance, the convectional patterns of PMMA spheres are similar to those of ethanol suspensions of colloidal silica spheres (110 nm in diameter) on a watch glass [7]. Several important findings are obvious in these figures. *Firstly*, clear and rather short spoke lines formed at the outside area of the liquid on a watch glass. The lines seemed to develop toward the central area, keeping similar distances between the nearest-neighbored spoke lines. Furthermore, the spoke lines diffused rapidly as they proceeded toward the central

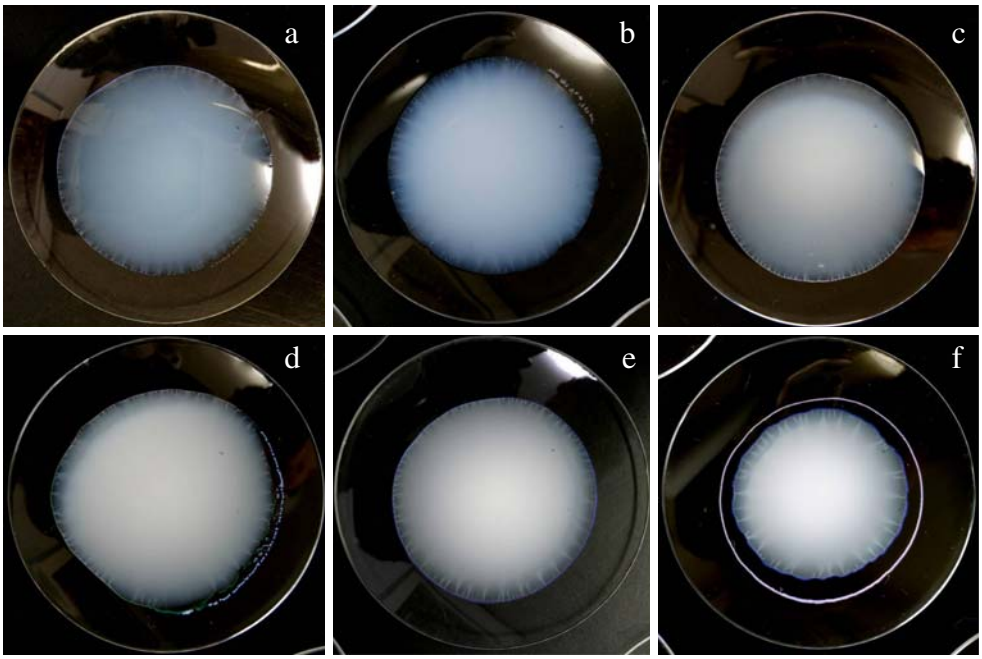

Fig. 1 Convectional patterns of GW1 (**a**, **b**), GW6 (**c**, **d**), and GW8 (**e**, **f**) spheres on a watch glass at 24°C. **a** ϕ=0.00095, 10 h 45 min after setting; **b** 0.00318, 14 h 25 min; **c** 0.00063, 15 min; **d** 0.0021, 15 min; **e** 0.00245, 17 h 15 min; **f** 0.00245, 24 h 55 min

area. It should be recalled that the spoke lines of PMMA spheres on a cover glass formed in a wide area from the outside edge to the center [51]. The liquid layers at the outside area on a watch glass will be very thin but comes deep (or thick) rapidly. Thus, the spoke lines must be visualized only at the outside area, since the water evaporation at the outside area is very significant at the thin liquid area. As Terada et al. [1–3] and the authors [6] observed the convectional patterns of Chinese black ink on water and on a glass dish, respectively, a large number of the very small convectional circles, *cell convections*, were formed to the normal direction of the spoke lines. It is highly plausible that every spoke line is composed of the valleys and hills with the upward and downward flow of the circular cell convections (see the schematic picture of Fig. 5(a) of [6]). Furthermore, the spoke lines, which were formed by the downward flow of spheres, were observed clearer than those by upward flow [6]. *Secondly*, the number of spoke lines was small at the initial stage of the growth of the spoke lines. However, the number increased with time and then turned to decrease passing the maximum number at the final stage of drying especially for GW1 spheres (see Fig. 2a). However, the spoke lines of GW6 and GW8 spheres appeared suddenly, and their numbers decreased monotonously with time. It should be mentioned here that very fine and short spoke lines further appeared suddenly in between the distinct spoke lines so far at the final stage of convectional pattern formation when the initial sphere concentrations of GW1 and GW6 spheres were from 0.001 to 0.003 in volume fraction. These features are shown in Fig. 2, where crosses and open triangles show the large spoke line numbers after around 25 h. For suspensions of GW8 spheres, several fine and short spoke lines appeared in between the distinct and long ones at the rather early stage of convectional pattern formation. As is further shown in Fig. 2, the spoke line numbers on a watch glass were rather insensitive to the initial sphere concentration, though the experimental errors were large. Furthermore, the spoke-line numbers at the initial stages increased as sphere size increased. These observations are similar to the observations on a cover glass [51].

Sedimentation and drying patterns on a watch glass

Figures 3, 4, 5, and 6 show the typical examples of the patterns formed during the course of dryness of the deionized suspensions of GW1, GW6, GW8, and PM1000 spheres, respectively. The patterns of GW1 spheres at ϕ= 0.00064 and 0.095 are shown in Fig. 3a–d and e–h, respectively. Sphere size of GW1 is so small (100 nm in diameter) that the sphere sedimentation did not take place as much as the whole course of dryness at any sphere concentrations examined. However, it is highly plausible that the broad ring-like accumulation of spheres took place in the outward liquid area (see the blue region in Fig. 3a), which is due to the difference in the rate of convectional flows between small amount of water and large spheres. Drying of the suspensions of GW1 spheres started clearly from the outside edge of the watch glass 17 h 50 min and 10 h 45 min after the suspensions were set at the low and high sphere concentrations, respectively (see Fig. 3). It should be mentioned here that the characteristic color changes took place during the course of dryness. As are

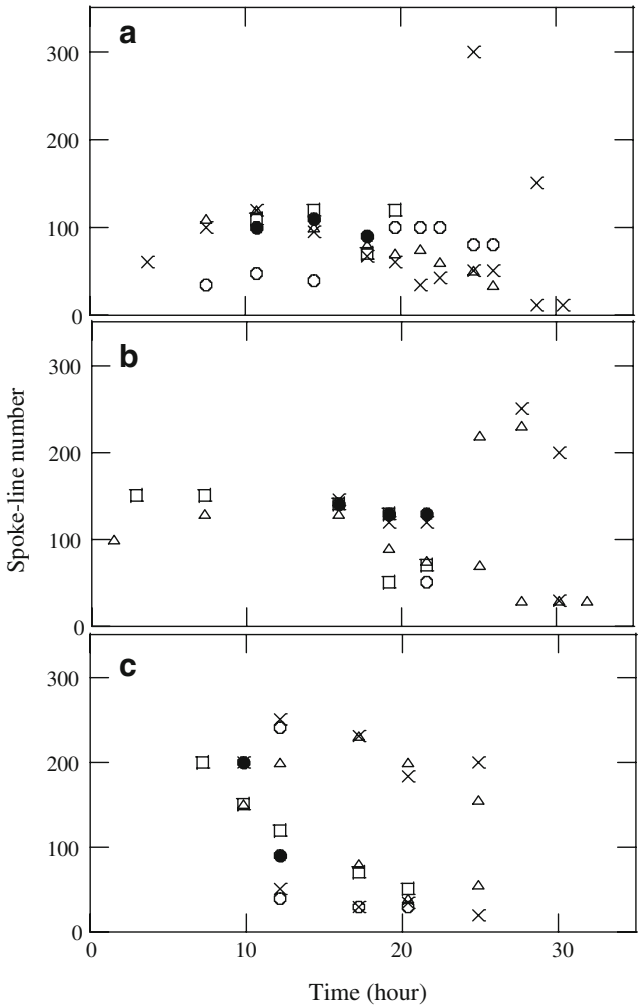

Fig. 2 Change in the spoke-like line number of GW1 (**a**), GW6 (**b**), and GW8 (**c**) with time on a cover glass. **a** *Open circle*, ϕ=0.000318; *Ex mark*, 0.00095; *open triangle*, 0.00318; *open square*, 0.0064; *closed circle*, 0.0159. **b** *Open circle*, ϕ=0.000210; *Ex mark*, 0.00063; *open triangle*, 0.00210; *open square*, 0.00420; *closed circle*, 0.0105. **c** *Open circle*, ϕ=0.000245; *Ex mark*, 0.00074; *open triangle*, 0.00245; *open square*, 0.00490; *closed circle*, 0.0123

shown in Fig. 3a–c, the liquid areas were bluish and white at the inner and outer areas. At the beginning stage of dryness, the color was whitish (see Fig. 3c), but changed again toward whitish blue at the stage of the completed dryness (see Fig. 3d). These changes in colors are due to the delicate change in the strength of the multiple scattering between wetted and dried films. It is highly plausible from our experiences that the crystal-like distribution of spheres is stable throughout the course of dryness from liquid to solid [33, 34]. The bluish colors are clearly from the Bragg diffraction of light by the crystal-like distribution of spheres. The primary peak wavelength (λp) in the reflection spectroscopy of colloidal crystals at the scattering angle of 90° is estimated from the nearest-neighbored intersphere distance (D) of the face-centered and/or body-centered cubic lattices.

$$\lambda p = nD/0.6124 \tag{1}$$

Here, the refractive indices of the liquid and dried film (n) are given by Eq. 2.

$$n = \phi x[\text{refractive index of PMMA sphere}] + (1-\phi) \times \begin{bmatrix} \text{refractive index of water} \\ \text{(for liquid andwetted film)or air(for dried film)} \end{bmatrix} \tag{2}$$

Refractive indices of PMMA, water, and air were assumed to be 1.49, 1.33, and 1.00, respectively. For the dried film, ϕ and D are 0.74 and diameter of spheres, respectively. Here, the spheres in the dried film were assumed to be attached to each other and distributed in the close-packed colloidal crystal structure. The λp values of the dried films are estimated to be 220, 430, and 650 nm and 2.2 μm for GW1, GW6, GW8, and PM1000 spheres, respectively. Depending on the scattering angles, color should change, but the color is estimated roughly to be blue

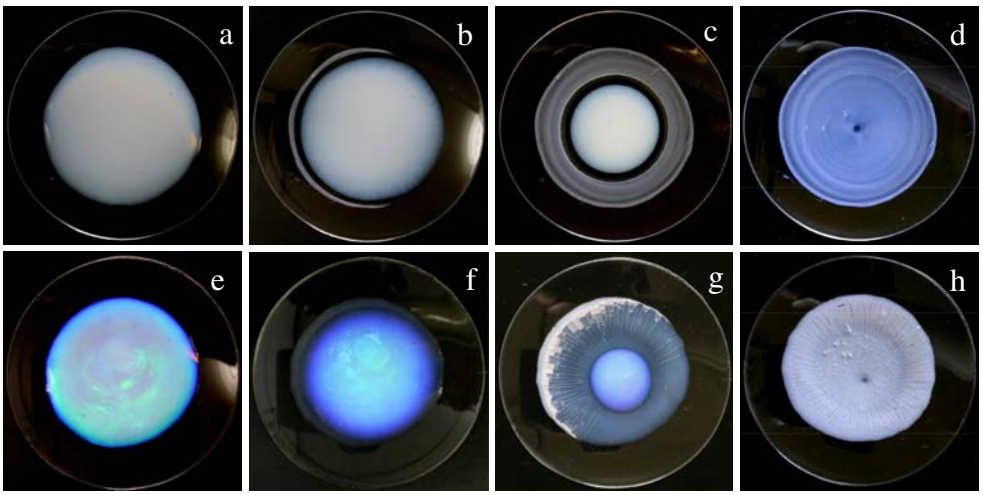

Fig. 3 Convectional, sedimentation, and drying patterns of GW1 spheres on a watch glass at 26°C. ϕ=0.00064 (**a**, **b**, **c**, **d**), 0.095 (**e**, **f**, **g**, **h**). **a** 55 min after setting; **b** 17 h 50 min; **c** 26 h; **d** 41 h 5 min; **e** 55 min; **f** 10 h 45 min; **g** 19 h 40 min; **h** 41 h 5 min

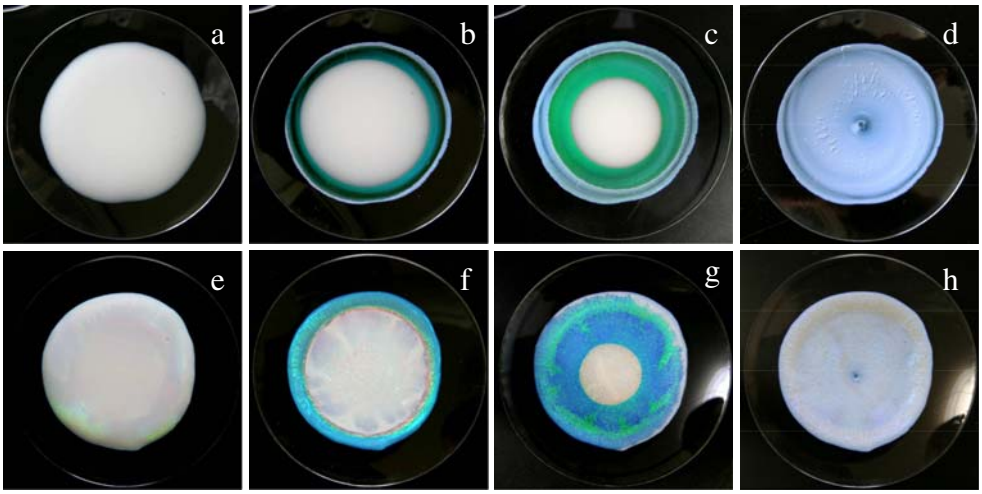

Fig. 4 Convectional, sedimentation and drying patterns of GW6 spheres on a watch glass at 24°C. ϕ=0.0105 (**a**, **b**, **c**, **d**), 0.063 (**e**, **f**, **g**, **h**). **a** 15 min after setting; **b** 25 h 5 min; **c** 30 h 15 min; **d** 42 h 10 min; **e** 15 min; **f** 21 h 40 min; **g** 27 h 50 min; **h** 42 h 10 min

(ultra-violet), green, red, and ultra-red (actually purely white by the very strong multiple scattering), respectively. For liquid state of suspensions, the λp values should be larger than those of the dried films. Thus, the observed colors of the suspensions of GW1 spheres, for example, at medium and high concentrations, and that of the dried film are understood to be green, blue, and whitish blue, respectively.

The multiple broad ring-like drying patterns were eventually observed at the low sphere concentrations of all the spheres examined, whereas single broad ring patterns were observed at the high sphere concentrations. Formation of these broad rings is clearly due to the strong convectional flow of spheres along the lower layers of the liquid toward the outside edges from the central area. It should be noted here that this convectional flow is strong enough to rise out of the colloidal spheres along the sloped planes of the substrate, i.e., the watch glass. The spheres in the drying patterns were vacant in the central areas at any sphere concentrations as are shown in Figs. 3, 4, 5, and 6. These holes have been observed so often hitherto on a watch glass, a cover glass, and also a glass dish [6–8, 11, 33, 34, 37, 43, 45, 46, 48, 49, 51]. Change in the patterns during the course of dryness of the suspensions of GW6 spheres were much colorful and beautiful compared with that of GW1 spheres (see Fig. 4). Furthermore, the multiple broad ring patterns at low sphere concentrations shifted again to the single broad ring as sphere concentration increased. The sedimentation patterns of GW6 spheres are shown in Fig. 4a–e. The beautifully colorful broad ring-like sedimentation pattern is seen in Fig. 4e. Figure 5a–h shows the typical patterns of convectional, sedimentation, and drying patterns of GW8 spheres. They are also colorful and beautiful. These colors are also explained nicely with Eqs. 1 and 2. The multiple broad rings and the single broad rings were observed again at the low and high sphere concentrations, respectively.

The drying patterns of colloidal crystals of GW1, GW6, GW8, and PM1000 were compared in Fig. 7a. Several important findings are noted. *Firstly*, colors of the dried

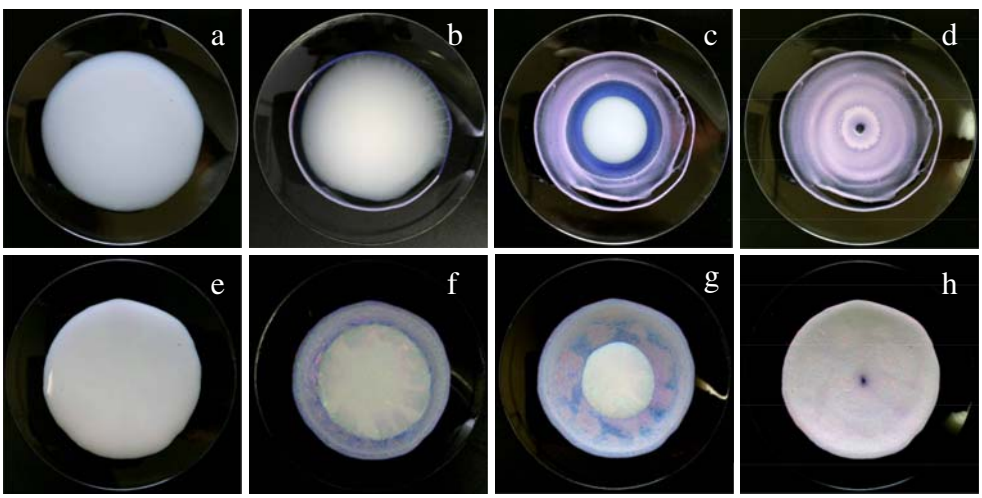

Fig. 5 Convectional, sedimentation, and drying patterns of GW8 spheres on a watch glass at 24°C. ϕ=0.0049 (**a**, **b**, **c**, **d**), 0.074 (**e**, **f**, **g**, **h**). **a** 30 min after setting; **b** 17 h 15 min, **c** 26 h 25 min; **d** 30 h 20 min; **e** 30 min; **f** 17 h 15 min; **g** 20 h 25 min; **h** 30 h 20 min

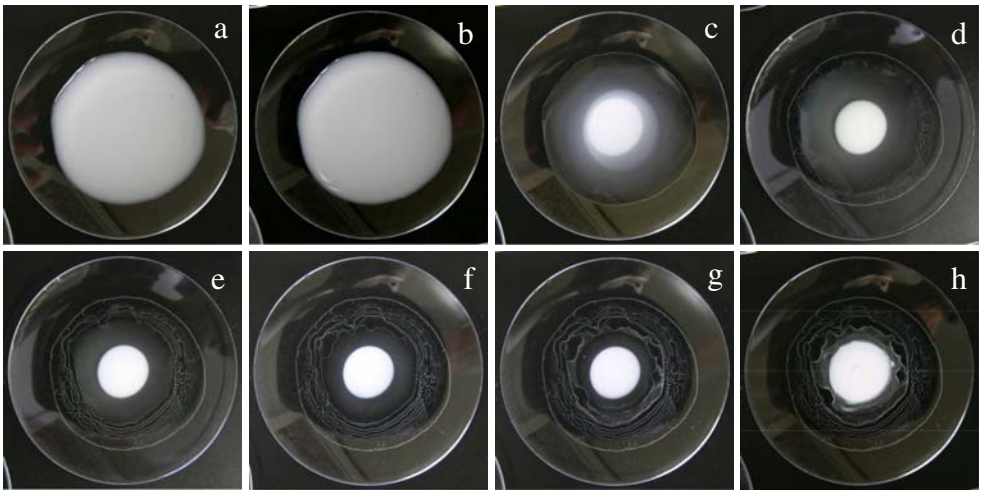

Fig. 6 Convectional, sedimentation and drying patterns of PM1000 spheres on a watch glass at 25°C. ϕ=0.00266. **a** 20 min after setting; **b** 55 min; **c** 6 h 20 min; **d** 15 h 40 min; **e** 22 h 5 min; **f** 24 h 30 min; **g** 26 h 5 min; **h** 27 h 25 min

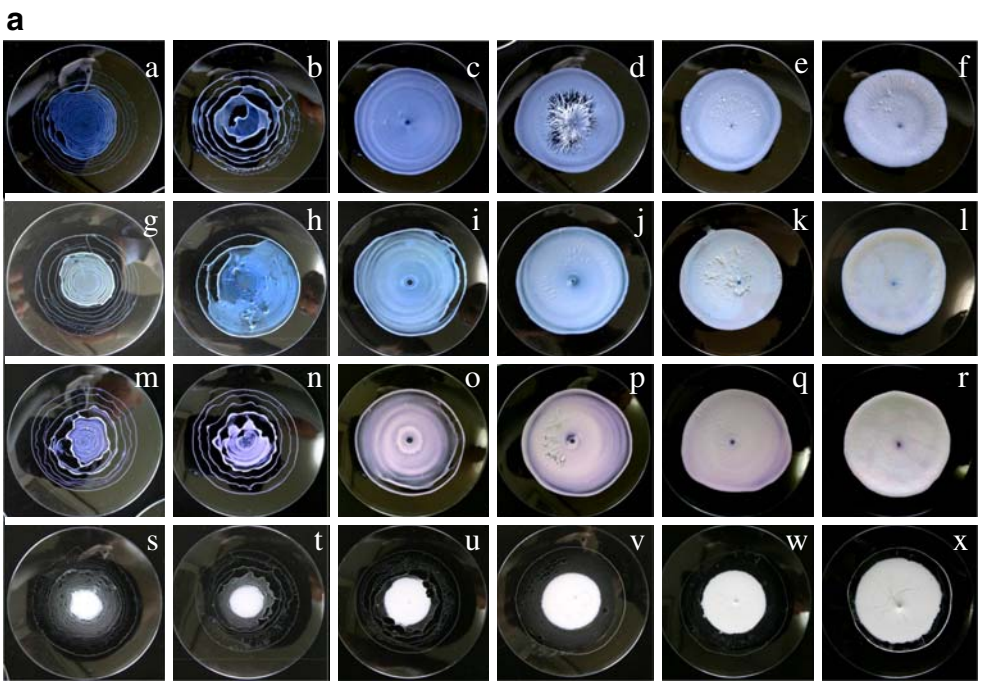

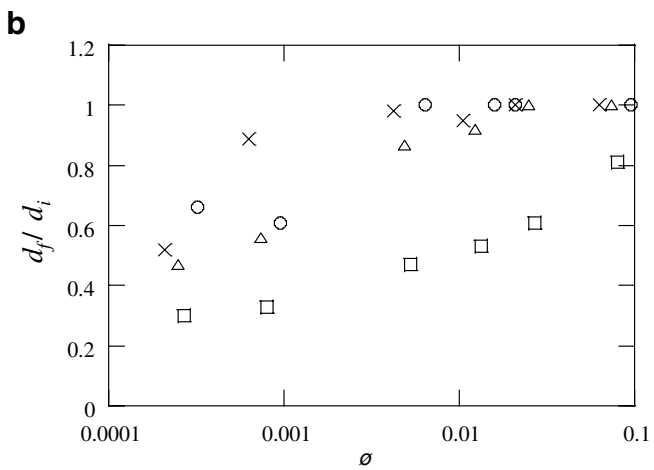

Fig. 7 **a** Drying patterns of PMMA spheres on a watch glass. *a* GW1, ϕ=0.00032; *b* 0.00095; *c* 0.0064; *d* 0.0159; *e* 0.021; *f* 0.095; *g* GW6, ϕ=0.00021; *h* 0.00063; *i* 0.0042; *j* 0.0105; *k* 0.021; *l* 0.063; *m* GW8, ϕ= 0.00025; *n* 0.00074; *o* 0.0049; *p* 0.0123; *q* 0.025; *r* 0.074, *s* PM1000, ϕ=0.00027; *t* 0.00080; *u* 0.0053; *v* 0.0133; *w* 0.027; *x* 0.080. **b** Change in the ratio *df*/*di* of GW1 (*open circle*), GW6 (*Ex mark*), GW8 (*open triangle*), and PM1000 (*open square*) as a function of sphere concentration ϕ

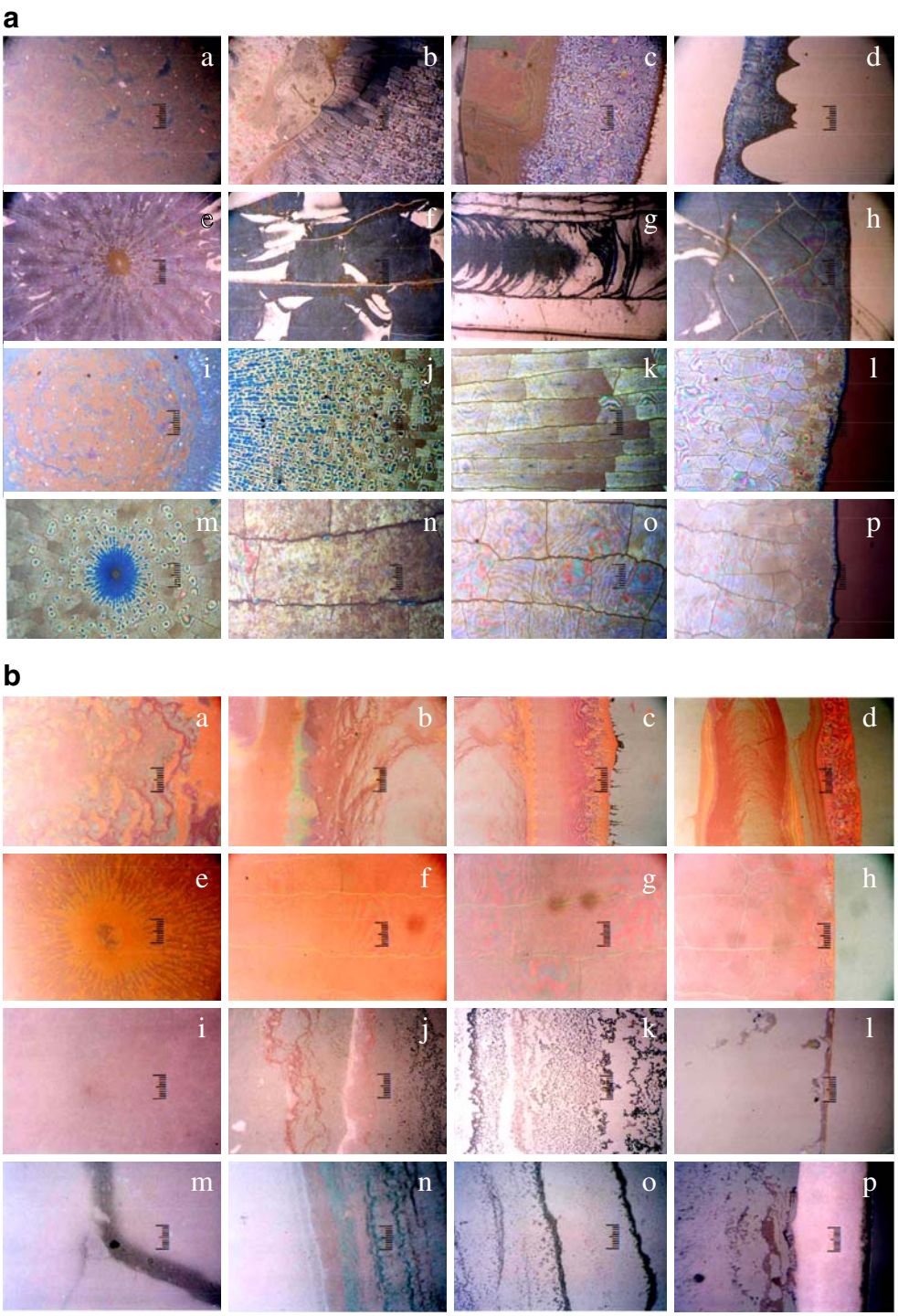

Fig. 8 **a** Microscopic drying patterns of PMMA spheres on a watch glass. *a–d* GW1, ϕ= 0.00095, *e–h* GW1, 0.095, *i–l* GW6, 0.0105, *m–p* GW6, 0.042; *from left to right*, the pictures *from central area to outside edge*, full scale= 200 μm. **b** Microscopic drying patterns of PMMA spheres on a watch glass. *a–d* GW8, ϕ= 0.00074; *e–h* GW8, 0.049; *i–l* PM1000, 0.00080; *m–p* PM1000, 0.053; *from left to right* the pictures *from central area to outside edge*, full scale=200 μm

films were blue, greenish blue, pink, and white for these spheres, respectively. Furthermore, these colors became whitish as initial sphere concentration increased. These findings were already discussed above with Fig. 3 and the Bragg equation. *Secondary*, at the low sphere concentrations, fine multiple rings were formed at the inner regions of the initial liquid areas. On the other hand, at the high sphere concentrations, the dried area did not shrink except PM1000 spheres. For PM1000 spheres, the main dried pattern area decreased significantly especially at the low sphere concentrations, which is due to the substantial sedimentation of the spheres toward central area. Figure 7b shows the ratios of the final dried pattern size in diameter against initial liquid size plotted against initial sphere concentration. Clearly, the ratios decreased as sphere size increased and/or sphere concentration decreased.

Thirdly, the holes where the spheres are vacant were observed at the central area of the dried film for all the spheres examined. The important role of the convectional flow of spheres through the liquid stages is again supported strongly. *Fourthly*, the macroscopic spoke lines (cracks) were observed especially for small GW1 spheres. The spoke lines disappeared when sphere size increased because the rigidity of the dried film decreases rapidly as sphere size decreases. These observations were also observed for the colloidal crystals of silica spheres [37].

Figure 8a and b show the microscopic dried patterns of the PMMA spheres on a watch glass at the typical low and high sphere concentrations. Colors of all the pictures observed with a microscope were slightly brownish and a bit different from those of the macroscopic patterns with a close-up camera. At the central areas, the holes and the very fine spoke-like crack lines were observed especially for the small spheres. These lines are originated from the traces of spheres by the convectional flow at the liquid step. Circle-like cracks were also observed, and crack cells composed of the spoke lines and circle lines are observable (see pictures n, k, o, and p of Fig. 8a). It should be further mentioned that the microscopic patterns changed delicately depending on sphere size and concentration. For large PM1000 spheres, clear-cut microscopic patterns were rather difficult to be observed. This is due to the very strong multiple-scattering of the incident light.

In conclusion, the convectional patterns were observed for the deionized suspensions of PMMA colloidal spheres on a watch glass and at room temperature in this work. It is impressive to observe the color changes during the course of dryness. Drying patterns of broad rings and spoke lines were observed so often in the present suspension systems.

Acknowledgments Financial support from the Ministry of Education, Culture, Sports, Science and Technology, Japan and Japan Society for the Promotion of Science are greatly acknowledged for Grants-in-Aid for Exploratory Research (17655046) and Scientific Research (B) (18350057). The PMMA sphere samples, GW1, GW6, GW8, and PM1000 were a gift from Soken Chemical (Tokyo), which the author appreciates very much.

References

1. Terada T, Yamamoto R, Watanabe T (1934) Proc Imp Acad (Tokyo) 10:10
2. Terada T, Yamamoto R, Watanabe T (1934) Sci Pap Inst Phys Chem Res Jpn 27:75
3. Terada T, Yamamoto R (1935) Proc Imp Acad (Tokyo) 11:214
4. Ball P (1999) The self-made tapestry formation in nature. Oxford University Press, Oxford
5. Fischer BJ (2002) Langmuir 18:60
6. Okubo T, Kimura H, Kimura T, Hayakawa F, Shibata T, Kimura K (2005) Colloid Polym Sci 283:1
7. Okubo T (2006) Colloid Polym Sci 285:225
8. Okubo T (2006) Colloid Polym Sci 284:1395
9. Okubo T (2006) Colloid Polym Sci 284:1191
10. Okubo T (2006) Colloid Polym Sci 285:331
11. Okubo T, Okamoto J, Tsuchida A (2007) Colloid Polym Sci 285:967
12. Okubo T (2007) Colloid Polym Sci 285:1495
13. Vanderhoff JW, Bladford EB, Carrington WK (1973) J Polym Sci Symp 41:155
14. Nicolis G, Prigogine I (1977) Self-organization in non-equilibrium systems. Wiley, New York
15. Cross MC, Hohenberg PC (1993) Rev Mod Phys 65:851
16. Adachi E, Dimitrov AS, Nagayama K (1995) Langmuir 11:1057
17. Ohara PC, Heath JR, Gelbart WM (1998) Langmuir 14:3418
18. Uno K, Hayashi K, Hayashi T, Ito K, Kitano H (1998) Colloid Polym Sci 276:810
19. Gelbart WM, Sear RP, Heath JR, Chang S (1999) Faraday Discuss Chem Soc 112:299
20. van Duffel B, Schoonheydt RA, Grim CPM, De Schryver FC (1999) Langmuir 15:957
21. Maenosono S, Dushkin CD, Saita S, Yamaguchi Y (1999) Langmuir 15:957
22. Brock SL, Sanabria M, Suib SL, Urban V, Thiyagarajan P, Potter DI (1999) J Phys Chem 103:7416
23. Nikoobakht B, Wang ZL, El-Sayed MA (2000) J Phys Chem 104:8635
24. Ge G, Brus L (2000) J Phys Chem 104:9573
25. Chen KM, Jiang X, Kimerling LC, Hammond PT (2000) Langmuir 16:7825
26. Lin XM, Jaenger HM, Sorensen CM, Klabunde KJ (2001) J Phys Chem 105:3353
27. Kokkoli E, Zukoski CF (2001) Langmuir 17:369
28. Ung T, Liz-Marzan LM, Mulvaney P (2001) J Phys Chem 105:3441
29. Haw MD, Gilli M, Poon WCK (2002) Langmuir 18:1626
30. Narita T, Beauvais C, Hebrand P, Lequeux F (2004) Eur Phys J E 14:287
31. Tirumkudulu MS, Russel WB (2005) Langmuir 21:4938
32. Shimomura M, Sawadaishi T (2001) Curr Opin Colloid Interface Sci 6:11
33. Okubo T, Okuda S, Kimura H (2002) Colloid Polym Sci 280: 454
34. Okubo T, Kimura K, Kimura H (2002) Colloid Polym Sci 280:1001
35. Okubo T, Kanayama S, Ogawa H, Hibino M, Kimura K (2004) Colloid Polym Sci 282:230
36. Okubo T, Kanayama S, Kimura K (2004) Colloid Polym Sci 282:486
37. Okubo T, Yamada T, Kimura K, Tsuchida A (2005) Colloid Polym Sci 283:1007
38. Yamaguchi T, Kimura K, Tsuchida A, Okubo T, Matsumoto M (2005) Colloid Polym Sci 283:1123
39. Kimura K, Kanayama S, Tsuchida A, Okubo T (2005) Colloid Polym Sci 283:898
40. Okubo T, Shinoda C, Kimura K, Tsuchida A (2005) Langmuir 21:9889
41. Okubo T, Yamada T, Kimura K, Tsuchida A (2006) Colloid Polym Sci 284:396
42. Okubo T, Itoh E, Tsuchida A, Kokufuta E (2006) Colloid Polym Sci 285:339
43. Okubo T, Nozawa M, Tsuchida A (2007) Colloid Polym Sci 285:827
44. Okubo T, Kimura K, Tsuchida A (2007) Colloids Surf 56:201
45. Okubo T, Onoshima D, Tsuchida A (2007) Colloid Polym Sci 285:999
46. Okubo T, Nakagawa N, Tsuchida A (2007) Colloid Polym Sci 285:1247

47. Okubo T, Yokota N, Tsuchida A (2007) Colloid Polym Sci 285:1257
48. Okubo T, Kimura K, Tsuchida A (2008) Colloid Polymer Sci 286:385
49. Okubo T, Kimura K, Tsuchida A (2008) Colloid Polymer Sci 286:621
50. Okubo T, Okamoto J, Tsuchida A (2008) Colloid Polymer Sci 286:941
51. Okubo T, Okamoto J, Tsuchida A (2008) Colloid Polymer Sci 286:1123
52. Palmer HJ (1976) J Fluid Mech 75:487
53. Anderson DM, Davis SH (1995) Phys Fluids 7:248
54. Routh AF, Russel WB (1998) AIChEJ 44:2088
55. Burelbach JP, Bankoff SG, Davis SH (1998) J Fluid Mech 195:463
56. Deegan RD, Bakajin O, Dupont TF, Huber G, Nagel SR, Witten TA (2000) Phys Rev E 62:756